

# CO Chemisorption and Hydrogenation of Surface Carbon Species Formed after CO/He Reaction on Rh/MgO: A Transient Kinetic Study Using FTIR and Mass Spectroscopy

A. M. Efstathiou,<sup>1,\*</sup> T. Chafik,<sup>†</sup> D. Bianchi,<sup>†</sup> and C. O. Bennett\*

\*Department of Chemical Engineering, University of Connecticut, Storrs, Connecticut 06269-3139; and <sup>†</sup>Laboratoire des Matériaux et Procédés Catalytiques, Université Claude-Bernard (Lyon I), ESCIL, 43 Boulevard du 11 Novembre 1918, 69622, Villeurbanne Cedex, France

Received September 21, 1993; revised November 17, 1993

The chemisorption of CO and hydrogenation of surface adsorbed carbon species formed after reaction of CO/He with Rh/MgO catalyst in the range 300–573 K were studied by transient methods employing both FTIR and mass spectroscopy in separate flow and reactor systems. Exposure of Rh/MgO to CO/He at 523 K results in a rapid formation of linear and bridged CO species. It was found that formation of gem-dicarbonyl CO species during CO chemisorption at 300 K is strongly affected by CO/He treatment at 523 K and H<sub>2</sub> reduction conditions. Experiments with labelled CO (<sup>13</sup>CO and C<sup>18</sup>O) indicate that linear and bridged CO species readily exchange with gaseous CO species. Transient hydrogenation results for adsorbed carbon-containing species formed after CO/He reaction at 523 K provide evidence that H<sub>2</sub> chemisorption decreases after cycles of reaction in CO/He at 523 K followed by H<sub>2</sub> reduction at 673 K. However, the surface coverages of adsorbed CO species are not affected by such treatments. Oxygen pretreatment of the catalyst at 623 K followed by H<sub>2</sub> reduction, after CO/He reaction at 523 K, greatly affects the transient kinetics of hydrogenation of adsorbed CO species at 523 K but not their respective surface coverages. This result is related to a change in the hydrogen chemisorption sites by oxygen treatment which resulted in the removal of inactive carbon not hydrogenated at 723 K. A kinetic model for the hydrogenation of the various adsorbed carbon-containing species is proposed which accounts for the interpretation of the CH<sub>4</sub> transient responses obtained. © 1994 Academic Press, Inc.

## INTRODUCTION

Transient methods have been used effectively in the last 10 years to measure *in situ* the surface coverages and reactivities of carbon-containing intermediate species formed after CO/H<sub>2</sub> reaction on Group VIII metal-supported catalysts (1–13). Studies related to measuring the composition of carbonaceous species formed after CO/He and after CO/H<sub>2</sub> reaction, under the same experimental conditions, can also provide useful information. For in-

stance, how the H<sub>2</sub> pressure affects the coverage of adsorbed CO and the coverage, as well as composition, of hydrogen-containing carbon species. These aspects have recently been studied over Rh/Al<sub>2</sub>O<sub>3</sub> (2, 3, 14) and in the past over Fe/Al<sub>2</sub>O<sub>3</sub> (15) and Ni/Al<sub>2</sub>O<sub>3</sub> (16) catalysts. In the aforementioned transient studies (1–12), the response of the catalyst surface to a step change imposed in the feed composition was measured by on-line mass spectrometry via the composition of gas-phase products which allowed the measurement of surface coverage of intermediate species. However, the chemical identity of surface intermediate species which are formed during reaction cannot always be obtained from gas-phase transient responses (3) or other transient titration experiments (15). Transient FTIR spectroscopy when used under appropriate experimental conditions can provide the means to *in situ* probe the chemical composition and surface dynamics of formation of intermediate species of a given reaction network. When transient FTIR is coupled with transient mass spectroscopy, the accuracy of characterizing a given surface reaction intermediate species is largely increased.

Even though transient FTIR spectroscopy has been used in the past for studying CO chemisorption and CO/H<sub>2</sub> reaction (13, 17–19), there is a limited work in this field using both transient FTIR and mass spectroscopy (20). These techniques have recently found application in the study of CO/H<sub>2</sub> reaction over 1wt% Rh/Al<sub>2</sub>O<sub>3</sub> (19) and 3wt% Rh/SiO<sub>2</sub> (13) catalysts. In the former case (19), it was possible to correlate transient responses obtained by FTIR with gas-phase transient responses obtained by mass spectrometry to measure the composition of the working surface of the Rh/Al<sub>2</sub>O<sub>3</sub> catalyst.

Recent infrared and EXAFS studies have shown that adsorption of CO on Rh crystallites at 300 K can lead to disruption of Rh–Rh bonds, resulting in the formation of gem-dicarbonyl CO species, Rh<sup>I</sup>(CO)<sub>2</sub> (18, 21–24). Basu *et al.* (25) first demonstrated the direct involvement of specific –OH groups of the oxide support in the formation

<sup>1</sup> Present address: Institute of Chemical Engineering and High Temperature Chemical Processes, GR-26500, Patras, Greece.

of gem-dicarbonyl CO species. It is important to know if the latter species is formed under CO/H<sub>2</sub> reaction conditions, and whether it truly participates in the formation of CH<sub>3</sub>OH and C<sub>2</sub>-oxygenates. The formation of these products from synthesis gas over Rh-supported catalysts has been related to the presence of oxidized rhodium (Rh<sup>n+</sup>) species (26).

Tanaka *et al.* (27) have studied by infrared spectroscopy the CO chemisorption over 2.3 wt% Rh/MgO catalyst, where linear and bridged CO were the only species observed. However, in the present study, under certain conditions, gem-dicarbonyl CO species, in addition to linear and bridged CO species, have been observed. These results, along with those mentioned in the previous paragraph, suggest that disruption of Rh crystallites by CO chemisorption does occur on the present Rh/MgO catalyst, as XPS results previously suggested (28), a phenomenon which has also been observed on Rh/Al<sub>2</sub>O<sub>3</sub> (18, 23–25).

The objectives of the present work were to study over a 2.5 wt% Rh/MgO catalyst (a) the CO chemisorption in the range 300–573 K, (b) the composition and kinetics of hydrogenation of surface carbon-containing intermediate species formed after CO/He reaction in the range 513–573 K, and (c) the effects of catalyst oxygen pretreatment on the aforementioned quantities (a) and (b). Transient experiments, as well as others with isotopes, using both FTIR and mass spectrometer as detectors have been conducted in separate flow and reactor systems. The results of this work are discussed in relation to those obtained for the CO/H<sub>2</sub> reaction over the present catalyst (4) and to those which have appeared in the literature related to this subject.

## EXPERIMENTAL

(a) *Catalyst.* A 2.5 wt% Rh/MgO catalyst was prepared by impregnating MgO (99.9% Aesar Co.) to incipient wetness (1.4 ml/g MgO) with an ethanol solution of RhCl<sub>3</sub> · 3H<sub>2</sub>O (Aldrich Chem. Co.) The BET area of the support (30 m<sup>2</sup>/g) and the active Rh metal surface area of the fresh catalyst (3.6 m<sup>2</sup>/g, fraction exposed FE = 0.3) were measured by N<sub>2</sub> adsorption and H<sub>2</sub> chemisorption, respectively, as described in detail elsewhere (14, 29). X-ray diffraction (XRD) showed no Rh (111) peak either for the fresh sample or for the sample after treatment with CO/He. No Mg(OH)<sub>2</sub> phase in the MgO was detected by XRD.

Transient experiments using mass spectrometry have been performed on a catalyst sample (0.3 g) which had already been used under CO/He atmosphere in the range 300–573 K for 3 h during characterization studies (29). At the end of these studies the catalyst achieved a reproducible activity towards CO chemisorption and hydroge-

nation. However, it was found that H<sub>2</sub> chemisorption decreased significantly from the value obtained on a fresh catalyst sample (29). The surface coverages reported in this work are based on 30 μmol Rh<sub>s</sub>/g cat as deduced by H<sub>2</sub> chemisorption on the present sample. Transient FTIR experiments have been conducted on a fresh catalyst sample (40 mg), which was pressed into a self-supporting disk of about 0.1 mm thickness and 21 mm diameter, in order to follow the effects of CO/He treatment on the CO chemisorption properties of the catalyst surface.

(b) *Reactor and flow-system.* Transient experiments using a mass spectrometer as detector were performed at 1 bar total pressure using a once-through stainless steel microreactor of 0.75 ml. The behaviour of this reactor was that of a CSTR (6). The flow system used for transient experiments has been described previously (6). The transient experiments using a FTIR spectrometer as detector were performed on another analytic system using a stainless steel FTIR cell of specific design, details of which were given elsewhere (30), with 1 ml internal volume. FTIR spectra can be recorded at the reaction temperature between 300 and 873 K and under a flow of gas varying in the range 150–300 cm<sup>3</sup>/min (ambient conditions).

The CO/He mixture used was 10 mol% CO and the CO in the <sup>13</sup>CO/He mixture had 99.3% <sup>13</sup>C. The transient results of CO exchange were corrected for the known concentrations of the various isotopes in the purchased <sup>13</sup>CO. The He and H<sub>2</sub> gases used were zero grade (Aero All-Gas Co.). Further purification of these gases was performed as described previously (6, 14). Gases were used at 1 bar total pressure and at a flow rate of 30 ml/min (ambient). The integrity of transient results, free of any flow disturbances during switching of valves, was maintained as described in (14, 31).

(c) *Mass and FTIR spectrometry.* Calibration and data acquisition of the high resolution mass spectrometer (Nuclide 12-90-G) responses obtained have been described in detail elsewhere (2, 14). Mass numbers used were 15, 28, and 29 for CH<sub>4</sub>, <sup>12</sup>CO, and <sup>13</sup>CO, respectively. The FTIR spectrometer used was of the model 5DX-C (Nicolet) with capabilities of recording one spectrum (averaged)/s using the SX software of the data acquisition system provided.

## RESULTS

The amount and chemical composition of the adsorbed carbon-containing species formed under CO/He reaction conditions over the Rh/MgO catalyst have been determined according to the following procedures: (1) isothermal and temperature programmed hydrogenation (TPR) to CH<sub>4</sub>, (2) FTIR in relation to their hydrogenation and exchange properties, and (3) exchange with gaseous <sup>13</sup>CO.

Mass spectrometry is used for the first and third experimental procedures.

(1) *Transient Hydrogenation of Adsorbed Carbon-Containing Species to CH<sub>4</sub>*

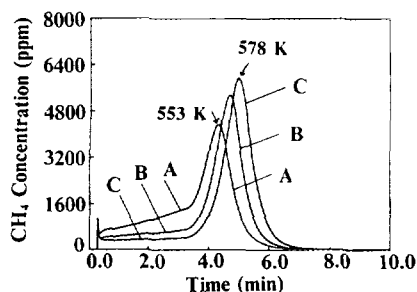
(1a) *Effects of reaction time in CO/He.* Figure 1 shows results of the transient hydrogenation of carbon-containing species formed after CO/He reaction at 523 K and for various times,  $\Delta t$ , on stream according to the following procedure. After reduction of the catalyst (see experimental section) in H<sub>2</sub> at 623 K and a 5-min He purge at 723 K, the reactor is cooled to 523 K. The feed is then changed to CO/He for a time of  $\Delta t = 60$  s, followed by a switch to pure H<sub>2</sub>. The CH<sub>4</sub> transient response obtained during the H<sub>2</sub> switch is given in Fig. 1, curve A, where no higher hydrocarbons were detected. It is noted that during the 60 s of CO/He reaction a CO<sub>2</sub> response is obtained due to the Boudouard reaction ( $2 \text{ CO(g)} \rightarrow \text{CO}_2\text{(g)} + \text{C(s)}$ ). The amount of carbon C(s) deposited on the surface was found to be small  $\theta_c = 0.01$  (based on the CO<sub>2</sub> response). In Fig. 1, curve A, there is a sharp increase in the rate of CH<sub>4</sub> formation as H<sub>2</sub> starts to flow over the catalyst. This is due to reduction of a very small amount of active carbon deposited during CO/He reaction, as stated above. As time on stream in H<sub>2</sub> increases, the rate of CH<sub>4</sub> production increases. After 3 min of isothermal reduction, the temperature is increased to perform a temperature-programmed reaction (TPR) in H<sub>2</sub> flow to 723 K. The heating rate used was 25 K/min. During this TPR experiment a CH<sub>4</sub> peak is formed with peak maximum,  $T_M$ , at 553 K. The reduction of all reactive carbonaceous species in H<sub>2</sub> is practically complete at about 700 K.

Results of the transient hydrogenation of carbon species formed after longer times on stream in CO/He at 523 K, such as 300 and 900 s, are given in curves B and C of Fig. 1, respectively. The amounts of carbon deposited based on the CO<sub>2</sub> response are  $\theta_c = 0.02$  and  $\theta_c = 0.05$ , respectively. The CO/He reaction corresponding to curve

B was performed following the H<sub>2</sub> TPR of curve A, and that corresponding to curve C following the H<sub>2</sub> TPR of curve B. It is observed that as time on stream in CO/He increases the rate of CH<sub>4</sub> formation during isothermal reduction decreases, and the  $T_M$  of the CH<sub>4</sub> peak formed under TPR increases. Note that the rate of CH<sub>4</sub> production increases during the first 3 min in H<sub>2</sub> at 523 K, as curves B and C indicate. Integration of the CH<sub>4</sub> transients in Fig. 1A–1C gives the amount of total carbonaceous species formed after a given reaction time in CO/He. This is found to be  $\theta = 1.15$ , 1.13, and 1.18 for 60, 300, and 900 s in CO/He, respectively. The value of  $\theta$  higher than one suggests that either chains of carbon are present on the metallic surface or a small quantity of adsorbed species is present on the MgO support contributing to the CH<sub>4</sub> production during the TPR process. The corresponding amounts obtained after 3 min of isothermal titration in H<sub>2</sub> are  $\theta = 0.40$ , 0.23, and 0.15. Thus, there is a significant decrease in the amount of surface CO which is hydrogenated at 523 K during a 3-min period of time as time on stream in CO/He increases. It is noted that during H<sub>2</sub> titration there is practically no CO desorption.

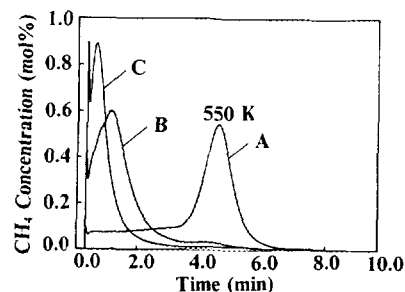
(1b) *Effects of temperature of hydrogenation.* Figure 2, curves A–C, shows results of the transient hydrogenation to CH<sub>4</sub> of carbon-containing species formed after reaction of the catalyst with CO/He for 10 min at 513, 553, and 573 K, respectively. It is observed that for the lowest reaction temperature studied (513 K, curve A), the CH<sub>4</sub> isothermal transient response and that obtained during TPR are similar to those observed after CO/He reaction at 523 K (Fig. 1). However, for higher reaction temperatures such as 553 and 573 K (Fig. 2, curves B and C, respectively) reduction of all carbon-containing species is almost complete within the first 3 min of isothermal reduction.

It is noted here that, for these two hydrogenation temperatures, after the initial sharp peak with a maximum at  $t = 0$  since H<sub>2</sub> is introduced over the catalyst, a second



CO/He  $\rightarrow$   $\rightarrow$  H<sub>2</sub>  $\rightarrow$  TPR

FIG. 1. Transient response of CH<sub>4</sub> according to the delivery sequence: CO/He (523 K,  $\Delta t$ )  $\rightarrow$  H<sub>2</sub> (523 K, 180 s)  $\rightarrow$  H<sub>2</sub> TPR. Curve A,  $\Delta t = 60$  s; curve B,  $\Delta t = 300$  s; curve C,  $\Delta t = 900$  s.



CO/He  $\rightarrow$   $\rightarrow$  H<sub>2</sub>  $\rightarrow$  TPR

FIG. 2. Transient response of CH<sub>4</sub> according to the delivery sequence: CO/He ( $T$ , 600 s)  $\rightarrow$  H<sub>2</sub> ( $T$ , 180 s)  $\rightarrow$  H<sub>2</sub> TPR. Curve A,  $T = 513$  K; curve B,  $T = 553$  K; curve C,  $T = 573$  K.

peak is observed with a maximum at  $t = t_m$  different from 0. This  $\text{CH}_4$  transient response is similar to that observed over other metal-supported catalysts such as Ru (32), Fe (33), and Ni (34) during hydrogenation of adsorbed carbon species formed after CO/He or CO/ $\text{H}_2$  reaction. In Fig. 2 it is observed that the second  $\text{CH}_4$  peak shifts to a higher value of  $t_m$  when the temperature decreases (compare curves B and C). At the temperature of 523 K (Fig. 1) and 513 K (Fig. 2, curve A) the  $t_m$  value of the maximum is higher than 3 min where only the beginning of the peak is well observed. Note also that in curve B a shoulder to the left appears. The presence of a shoulder and the shift in the time of appearance,  $t_m$ , of the second  $\text{CH}_4$  peak maximum described above is discussed later based on kinetic models (35–37, 44). The total amount of carbon species removed by  $\text{H}_2$  corresponding to the results of Fig. 2 is  $\theta = 1.3, 1.28,$  and  $1.1$  for 513, 553, and 573 K, respectively.

(1c) *Stability of adsorbed carbon species in He flow.* The stability of surface carbon-containing species in He flow at 523 K, after they are formed during CO/He reaction with the catalyst at 523 K for 300 s, was studied as follows. After the catalyst had been treated with CO/He, the feed was changed to  $\text{H}_2$  for 60 s, followed by a He purge for 60 s or 600 s, followed by a second switch to  $\text{H}_2$  (isothermal + TPR). Figure 3, curves a and b, show  $\text{CH}_4$  transient responses obtained during both  $\text{H}_2$  switches and for He purge times,  $\Delta t$ , of 60 and 600 s, respectively. The  $\text{CH}_4$  response obtained during the 60 s of the first  $\text{H}_2$  switch is that seen in Fig. 1, curve B. During He purge the reaction is quenched and small amounts of CO desorb. At the second  $\text{H}_2$  switch, following that of He purge, the rate of  $\text{CH}_4$  formation is very similar to that obtained at the end of the first  $\text{H}_2$  switch. The spike at the second  $\text{H}_2$  switch is due to a very small amount of active carbon formed by the dissociation of CO during He purge. A TPR experiment, following the isothermal reduction step,

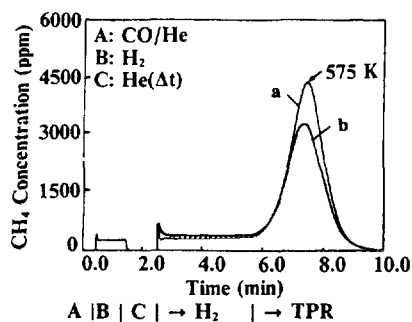


FIG. 3. Transient response of  $\text{CH}_4$  according to the delivery sequence: CO/He (523 K, 300 s)  $\rightarrow$   $\text{H}_2$  (523 K, 60 s)  $\rightarrow$  He (523 K,  $\Delta t$ )  $\rightarrow$   $\text{H}_2$  (523 K, 180 s)  $\rightarrow$   $\text{H}_2$  TPR. Curve a,  $\Delta t = 60$  s; curve b,  $\Delta t = 600$  s.

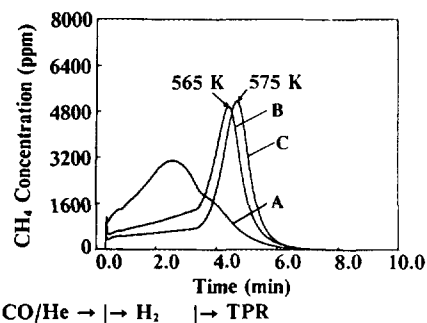


FIG. 4. Effects of catalyst oxygen treatment on the transient hydrogenation to  $\text{CH}_4$  of the adsorbed carbon species formed after CO/He reaction at 523 K. Curve A: the catalyst is first treated with  $\text{O}_2$  at 623 K for 30 min, followed by  $\text{H}_2$  reduction at 623 K for 2 h, followed by CO/He reaction at 523 K for 60 s. Curve B: at the end of the  $\text{H}_2$  TPR of curve A, the catalyst is purged in He at 623 K for 5 min and then cooled in He to 523 K followed by CO/He reaction for 300 s. Curve C: at the end of the  $\text{H}_2$  TPR of curve B the catalyst is purged in He at 623 K for 5 min and then cooled in He to 523 K followed by CO/He reaction for 900 s.

largely increases the rate of hydrogenation of the adsorbed carbon species to form  $\text{CH}_4$ .

On increasing the time of He purge at 523 K to 600 s (Fig. 3, curve b), the rate of  $\text{CH}_4$  production during the second  $\text{H}_2$  switch remains practically the same as that obtained for the case of 60 s of He purge (note the small increase of the initial sharp peak). However, the amount of carbon species removed by TPR (curve b) is somewhat less than that obtained for the case of 60 s of He purge ( $\theta = 0.96$  vs 1.05). This is due to the low rates of desorption and dissociation of CO.

(1d) *Oxygen pretreatment effects on the kinetics of hydrogenation of carbon-containing species formed after CO/He reaction at 523 K.* The effects of oxygen treatment of the Rh/MgO surface on the coverages of carbon species formed after CO/He reaction, as well as on the kinetics of hydrogenation of the latter species, are shown in Fig. 4. These results have been obtained according to the following experimental sequence. The catalyst was first treated with oxygen at 623 K for 30 min followed by hydrogen at 623 K for 2 h. A He purge was then applied at 723 K for 10 min followed by cooling of the reactor to 523 K. The feed was then changed to CO/He for 60 s, followed by  $\text{H}_2$  titration (isothermal + TPR). The  $\text{CH}_4$  transient response obtained during  $\text{H}_2$  titration is shown in Fig. 4, curve A. This response is much different from that obtained without any oxygen pretreatment of the catalyst (Fig. 1, curve A). Much of the carbon species formed after CO/He treatment, following the oxygen pretreatment described above, are reduced in  $\text{H}_2$  at 523 K during the first 3 min of titration, producing a  $\text{CH}_4$  peak at  $t_m = 130$  s on stream in  $\text{H}_2$ . This behaviour is not

observed in Fig. 1, curve A, where the  $t_m$  value is larger than 3 min. However, despite these large differences in the kinetics of hydrogenation of carbon species, the amount of these species is found to be independent of the catalyst oxygen pretreatment ( $\theta = 1.1$ ). It should be noted here that during  $O_2$  treatment  $CO_2$  is formed. This result is used later to discuss the behaviour of the transient hydrogenation responses of Fig. 4.

After the  $H_2$  titration step shown in Fig. 4, curve A, the catalyst is purged under He to 723 K and then cooled to 523 K. The feed is then changed to CO/He for 300 s followed by  $H_2$  reduction, as for the case of 60 s CO/He treatment. The  $CH_4$  transient response obtained (Fig. 4, curve B) appears now much different than that of curve A, but similar to that of Fig. 1, curve B (without catalyst oxygen pretreatment); there is a  $CH_4$  peak during the isothermal reduction step with a  $t_m$  larger than 3 min. Following the same gas treatments after the end of the experiment of curve B, as those corresponding to the experiment of curve A, CO/He is then passed over the catalyst for 900 s followed by  $H_2$  titration. Figure 4, curve C, gives the  $CH_4$  transient response obtained which is very similar to that observed in Fig. 1, curve C (without catalyst oxygen pretreatment). It is noted that the amount of carbon species formed after 60, 300 and 900 s of CO/He reaction given by curves A, B, and C of Fig. 4, respectively, is the same ( $\theta = 1.1$ ).

## (2) FTIR Analysis of Adsorbed Carbon Species

(2a) *Effects of time and temperature in CO/He.* The chemisorption of CO and its reaction with the surface of Rh/MgO at 523 K as a function of time on stream in CO/He was studied by in-situ FTIR spectroscopy. Figure 5,

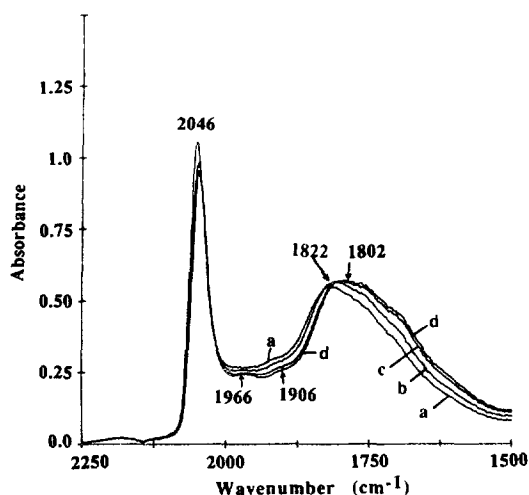


FIG. 5. Transient FTIR spectra in the range 1500–2250  $cm^{-1}$  recorded at 523 K during CO/He reaction over a reduced Rh/MgO surface. (a) 30 s; (b) 300 s; (c) 1200 s; (d) 3600 s.

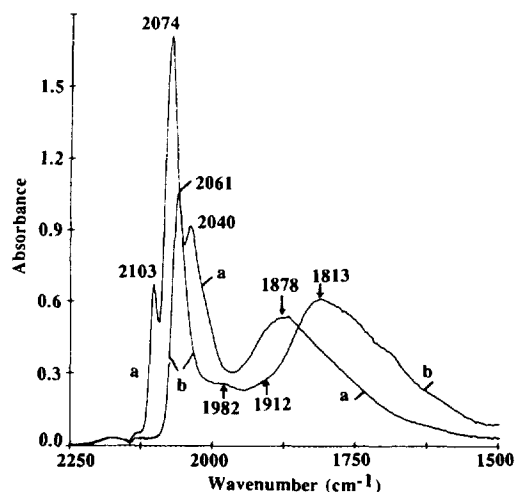


FIG. 6. Comparison of FTIR spectra in the range 1500–2250  $cm^{-1}$  obtained after chemisorption of CO at 300 K (spectrum a) over a reduced fresh Rh/MgO sample, and after CO/He reaction at 523 K for 1 h followed by cooling in CO/He to 300 K (spectrum b).

curves a–d, shows IR bands in the range 1500–2250  $cm^{-1}$  after reaction with 10% CO/He for 60, 300, 1200, and 3600 s, respectively. The fresh catalyst sample before reaction was reduced in  $H_2$  at 723 K for 1 h and purged under He for 5 min. After 60 s on stream, IR bands were recorded at 2046 and 1822  $cm^{-1}$  with a shoulder at 1966 and 1906  $cm^{-1}$ . The asymmetric character of the IR band at 1822  $cm^{-1}$  indicates that more than one IR band contributes to the IR absorption, and a shoulder around 1750  $cm^{-1}$  may be considered. For longer times on stream, the 2046  $cm^{-1}$  band (linear CO species, see discussion) stays almost constant, but the broad band at 1822  $cm^{-1}$  (bridged CO species, see discussion) shifts to 1802  $cm^{-1}$ , and the shoulder appeared at 1750  $cm^{-1}$  increases slightly, while its position may be considered at 1690  $cm^{-1}$ . FTIR data obtained in the range 473–573 K show that the coverages of the CO adsorbed species change very little, in agreement with the measurements performed by  $H_2$  titration (Figs. 1 and 2).

Of interest in the present study was to compare the chemisorption of CO at 300 K on a fresh sample and that on a sample first treated with CO/He at 523 K for a long period of time (1 h). Figure 6 shows these results. Spectrum a is obtained after a fresh catalyst sample is treated with CO/He at 300 K for 60 s, following reduction in  $H_2$  for 1 h and a 5-min He purge at 623 K. Spectrum b is obtained after the same catalyst pretreatment as for spectrum a is applied, followed by CO/He reaction for 1 h at 523 K and cooling in CO/He to 300 K. Spectrum b is similar to the spectra shown in Fig. 5, while only small shifts in the IR band positions are observed; these shifts are due to differences in the temperature. However, large changes are recorded in the two spectra of Fig. 6. In

spectrum a new IR bands at 2103 and 2040  $\text{cm}^{-1}$  (gem-dicarbonyl CO species associated with  $\text{Rh}^{+1}$ , see discussion) are recorded, while the linear and bridged CO species give IR bands at other positions (2074 and 1878  $\text{cm}^{-1}$ , respectively). The shoulders at 1982 and 1912  $\text{cm}^{-1}$  in spectrum b are not observed in spectrum a, whereas the IR band at 1878  $\text{cm}^{-1}$  is symmetrical in spectrum a but not in spectrum b. In addition, even after 1 h on stream in CO/He at 300 K, the gem-dicarbonyl CO species does not appear in the case of spectrum b. Thus, the main results are that CO/He treatment at 523 K leads to the disappearance of the sites which give rise to the formation of gem-dicarbonyl CO species, and to the formation of new species with IR bands at 1982, 1912, and 1750  $\text{cm}^{-1}$ .

The aforementioned changes in the CO chemisorption properties of Rh particles with respect to the adsorption temperature may be followed using the TPD technique. Figure 7A, spectrum a, gives the FTIR response recorded after adsorption of CO at 300 K from the CO/He mixture on a fresh catalyst sample. Spectrum b is recorded after 5 min of He purge, and spectra a–c in Fig. 7B are recorded at various temperatures during TPD (10 K/min). It is observed that removal of gaseous CO leads to a shift of the linear and bridged CO bands without change in the position of the gem-dicarbonyl CO bands. These phenomena become even more important at higher temperatures, where a strong overlap of the IR bands due to the linear CO and that at 2040  $\text{cm}^{-1}$  due to the gem-dicarbonyl CO species occurs. It is also observed that between 300 and 423 K the gem-dicarbonyl CO species disappear (band at 2100  $\text{cm}^{-1}$ ), whereas an IR band at 1918  $\text{cm}^{-1}$  appears.

The appearance at 423 K of the shoulder at 1750  $\text{cm}^{-1}$  makes the IR band of the bridged CO species nonsymmetrical. It seems that these shoulders correlate with the disappearance of the gem-dicarbonyl CO species. In addition, the shoulder at 1906  $\text{cm}^{-1}$  in Fig. 5 is formed at around 473 K. The increase of the temperature until 623 K leads to the disappearance of the FTIR bands associated to the production of CO and  $\text{CO}_2$  (29).

The effects of consecutive cycles of reaction in CO/He at 523 K, followed by  $\text{H}_2$  reduction at 623 K, on the chemisorption of CO at 523 K are presented in Fig. 8. Spectrum a is obtained after the fresh catalyst sample is reduced in  $\text{H}_2$  at 623 K followed by reaction in CO/He at 523 K for 1 h. At the end of this experiment, the catalyst is reduced in  $\text{H}_2$  at 623 K, followed by another CO/He treatment at 523 K for 1 h. Spectrum b is then obtained. These results clearly show that the kind of adsorbed CO species formed at 523 K (mainly linear and bridged) and their amounts do not depend on further CO/He treatment after the catalyst is first exposed to CO/He for 1 h.

(2b) *Stability of adsorbed carbon species in He flow.* The stability of adsorbed carbon species formed after CO/He reaction in He flow is presented in Fig. 9. After 30 min of CO/He reaction at 523 K over the  $\text{H}_2$  pretreated Rh/MgO sample, a switch from CO/He to He is made. Curves a–e give the changes in the IR spectrum obtained after various times in He. It can be observed that the linear (IR band at 2046  $\text{cm}^{-1}$ ) and the bridged (IR bands at 1815  $\text{cm}^{-1}$ ) CO species desorb slowly. The decrease of their coverages leads to a shift in the corre-

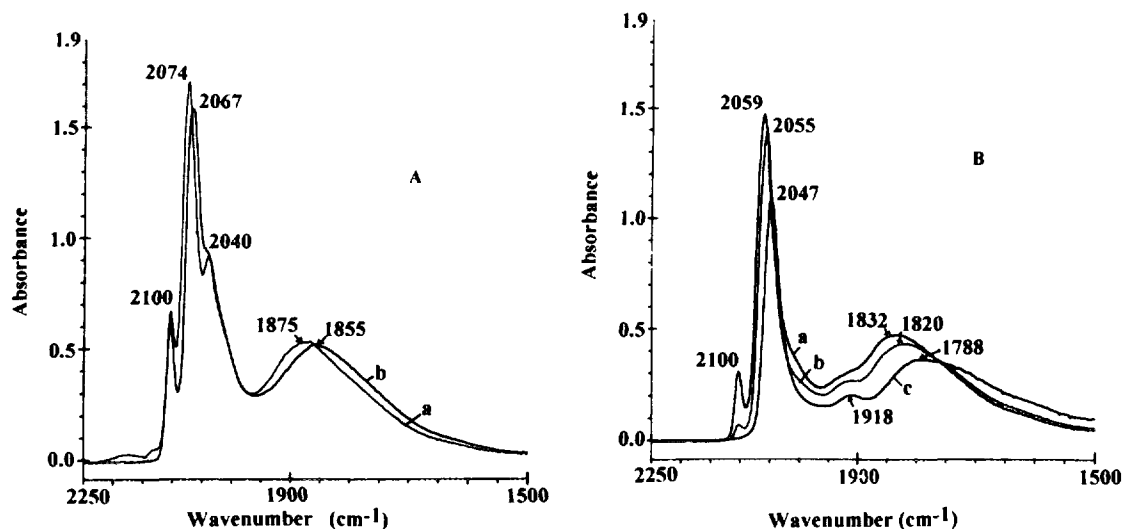


FIG. 7. (A) FTIR spectra in the range 1500–2250  $\text{cm}^{-1}$  recorded during chemisorption of CO at 300 K and 300 s on stream (spectrum a), and after 100 s of He purge at 300 K (spectrum b). (B) FTIR spectra in the range 1500–2250  $\text{cm}^{-1}$  recorded during He TPD after CO chemisorption at 300 K for 300 s. Spectrum (a) is obtained at 373 K, spectrum (b) at 408 K, and spectrum (c) at 423 K. CO chemisorption was performed on a fresh catalyst sample reduced at 623 K for 2 h.

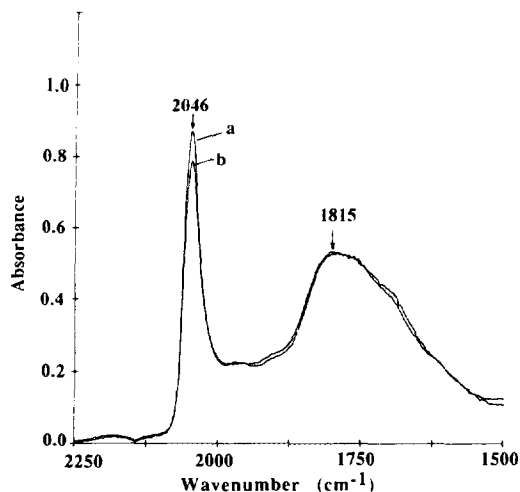


FIG. 8. Effects of consecutive cycles of reaction in CO/He at 523 K, followed by H<sub>2</sub> reduction at 623 K, on the chemisorption of CO. FTIR spectrum (a) is obtained after the fresh catalyst sample is reduced in H<sub>2</sub> followed by CO/He reaction for 1 h. FTIR spectrum (b) is recorded following H<sub>2</sub> reduction and 1 h CO/He reaction after spectrum (a) is obtained.

sponding bands to lower positions. The disappearance and shift of the bridged CO species make it possible to observe more clearly the initially produced shoulders at 1906 cm<sup>-1</sup> (shift to 1894 cm<sup>-1</sup> after 1520 s in He) and 1697 cm<sup>-1</sup> (shift to 1648 cm<sup>-1</sup> after 1520 s in He). The adsorbed species leading to those IR bands are more stable than the linear and bridged CO species. The initial shoulder at 1966 cm<sup>-1</sup> seems to decrease quickly within the first minute of He purge.

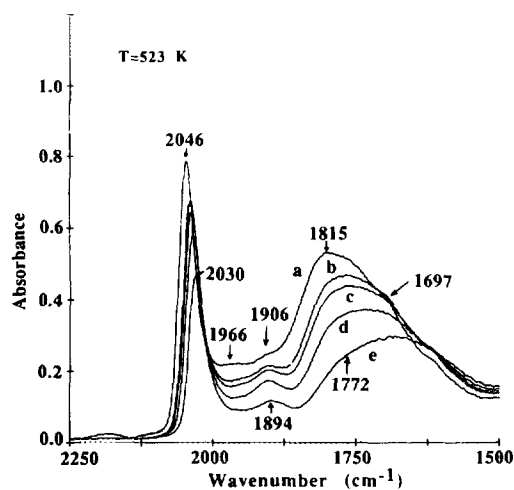


FIG. 9. FTIR spectra in the range 1500–2250 cm<sup>-1</sup> recorded at 523 K during a He isothermal desorption according to the sequence: CO/He (523 K, 30 min) → He (523 K, *t*) (a) *t* = 0 s; (b) *t* = 20 s; (c) *t* = 60 s; (d) *t* = 360 s; (e) *t* = 1520 s.

(2c) *Hydrogenation of adsorbed carbon species.* The isothermal hydrogenation at 523 K of adsorbed CO species formed after CO/He reaction at 523 K for 60 s was studied by FTIR after various times in H<sub>2</sub> flow. Figure 10, spectra a–e shows IR bands in the range 1500–2250 cm<sup>-1</sup> as recorded after 0, 20, 60, 140, and 240 s in H<sub>2</sub> flow. During the first 4 min in H<sub>2</sub>, the coverage of linear CO (band at 2046 cm<sup>-1</sup>, *t* = 0) and bridged CO species (band at 1815 cm<sup>-1</sup>, *t* = 0) decreases. This result indicates that the rate of hydrogenation of these species is larger than the rate of desorption (Fig. 9). The shift of their positions is similar to that observed in Fig. 9, and this is more related to the decrease of the surface coverage than to any hydrogen interactions. As for the desorption case in He (Fig. 9), the disappearance of the bridged CO species leads to the clear observation of the formation of shoulders at 1894 and 1648 cm<sup>-1</sup>. This result implies that the species responsible for these IR bands are hydrogenated with a lower rate than the linear or bridged CO species. The increase of the temperature from 523 to 573 K (15 K/min) results in the complete disappearance of the adsorbed carbon species (curves f–h). It is important to note here that neither CH<sub>x</sub> nor CH<sub>x</sub>O IR bands are detected during hydrogenation (Fig. 10). This result is discussed later in relation to the mechanism of hydrogenation of carbon species formed after CO/He reaction.

(2d) *Effects of catalyst pretreatment in oxygen.* The experiments described in Fig. 4, curves A–C, have also been performed using transient FTIR as follows. The catalyst sample disk was first treated with oxygen as described previously in the case of the catalyst sample used with

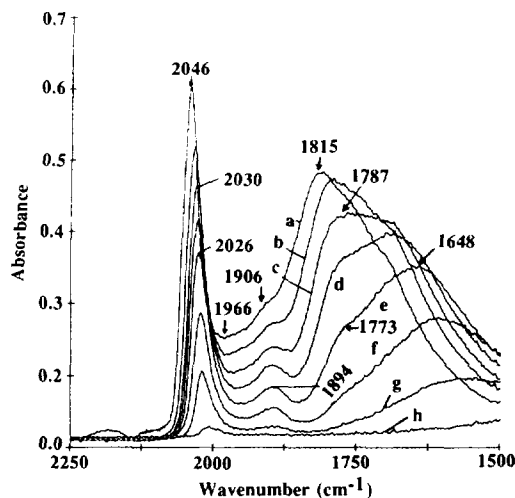


FIG. 10. FTIR spectra in the range 1500–2250 cm<sup>-1</sup> recorded between 523 K and 573 K during hydrogenation of adsorbed carbon species formed after CO/He reaction at 523 K. Delivery sequence: CO/He (523 K, 60 s) → H<sub>2</sub> (523 K, *t*) → H<sub>2</sub> TPR. (a) *t* = 0 s; (b) *t* = 20 s; (c) *t* = 60 s; (d) *t* = 140 s; (e) *t* = 240 s; (f) *T* = 538 K; (g) *T* = 553 K; (h) *T* = 573 K.

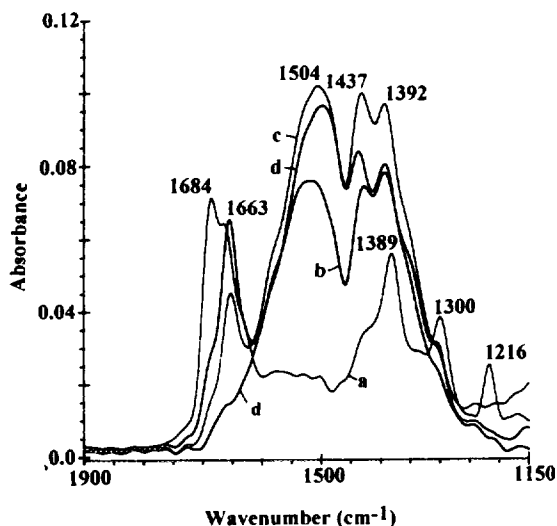


FIG. 11. FTIR spectra in the range 1150–1900  $\text{cm}^{-1}$  recorded between 320 K and 523 K during CO adsorption on MgO alone. Before CO chemisorption the MgO surface had been treated with  $\text{H}_2$  at 723 K for 1 h. Spectrum (a)  $T = 320$  K; (b)  $T = 405$  K; (c)  $T = 458$  K; (d)  $T = 523$  K.

mass spectrometry (Fig. 4, curve A). The spectrum taken after CO/He treatment at 523 K for 60 s was the same as that obtained without oxygen pretreatment (Fig. 5, spectrum a). This result clearly indicates that the kinds of adsorbed CO species and their coverages are not affected by an oxygen pretreatment. Thus, the transient hydrogenation results of Fig. 4 must be explained taking into account other kinetic factors which were influenced by the oxygen treatment applied. This aspect is discussed later.

(2e) *Adsorption of CO on the support alone.* To consider the chemisorption of CO on the support alone, adsorption results of CO at various temperatures on MgO pretreated with  $\text{H}_2$  at 723 K for 1 h followed by a 5-min He purge are shown in Fig. 11. At 300 K there are only very weak IR bands which increase with time in CO/He. The same behaviour is observed with increasing adsorption temperature (Fig. 11, curves a and b for 320 and 405 K, respectively), while the IR bands are still weak compared to those observed on Rh/MgO (Fig. 5, curve c). For higher temperatures, IR bands at 1684 and 1216  $\text{cm}^{-1}$  appear ( $T = 458$  K, Fig. 11, curve c), whereas the intensity of bands at 1504, 1437, and 1392  $\text{cm}^{-1}$  increases but remains weak. At 523 K (curve d), the IR bands at 1663 and 1300  $\text{cm}^{-1}$  are not detected, whereas above 523 K the intensity of the three remaining IR bands starts to decrease. At 493 K a switch to He leads to the fast disappearance of the 1663 and 1300  $\text{cm}^{-1}$  bands. By comparing the results in Figs. 5 and 11, the following points are noted: (a) the intensities of the IR bands recorded on MgO alone are about 10 times smaller than those observed

on the Rh/MgO, and (b) at  $T > 523$  K no adsorbed species on the MgO alone give IR bands higher than 1500  $\text{cm}^{-1}$ . These results show that direct adsorption of CO on the MgO cannot contribute significantly to the IR bands observed on Rh/MgO. It is not the objective of the present work to interpret the relatively complex FTIR spectrum recorded during CO interaction with the MgO surface. Previous work has shown that on pretreated MgO under inert conditions and high temperatures, such as  $T = 700$  K (38) or  $T = 1073$  K (39), adsorption of CO at 300 K leads to a complex IR spectrum. This result was interpreted as due to the formation of various carbonate species (38, 39). In the present study the pretreatment applied is different and leads to other IR bands. However, all the IR bands recorded (Fig. 11) are in the expected range of carbonate species.

### (3) Exchange Reaction with Gaseous $^{13}\text{CO}$

(3a) *Mass spectrometry analysis.* The steady-state tracing technique (1, 3) has been applied to *in situ* measure the surface coverage of CO species formed after reaction of Rh/MgO with CO/He at 523 K. The experiment was as follows. After allowing CO/He to flow over the catalyst at 523 K for 60 s, the feed was changed to  $^{13}\text{CO}/\text{He}$ , while at the same time the  $^{13}\text{CO}$  signal was followed by on-line mass spectrometry. The  $^{13}\text{CO}(\text{g})$  transient response

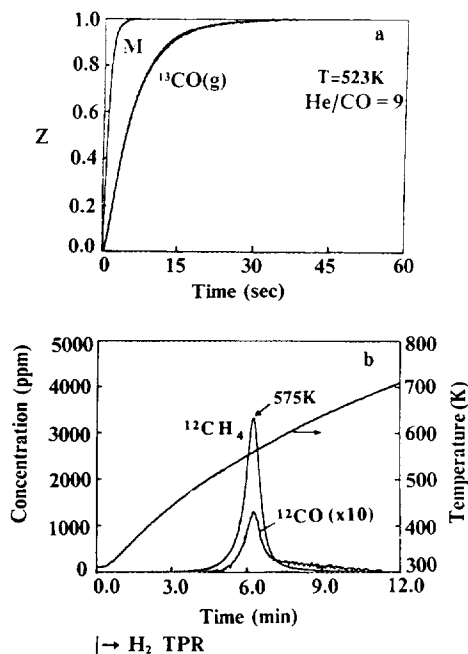


FIG. 12. (a) Transient isotopic exchange experiment of CO according to the delivery sequence:  $^{12}\text{CO}/\text{He}$  (523 K, 60 s)  $\rightarrow$   $^{13}\text{CO}/\text{He}$  (523 K,  $t$ ).  $Z$  is a dimensionless gaseous response defined in the text. (b)  $^{12}\text{CH}_4$  and  $^{12}\text{CO}$  responses obtained during  $\text{H}_2$  TPR according to the delivery sequence:  $^{12}\text{CO}/\text{He}$  (523 K, 60 s)  $\rightarrow$   $^{13}\text{CO}/\text{He}$  (523 K, 60 s)  $\rightarrow$  He(523 K, 15 s)  $\rightarrow$  cool to 313 K  $\rightarrow$   $\text{H}_2$  TPR.



obtained is given in Fig. 12a.  $Z$  is a dimensionless concentration given by

$$Z(t) = (y(t) - y_{\infty}) / (y_{\infty} - y_0), \quad [1]$$

where the subscripts 0 and  $\infty$  refer to values of  $y$  (mole fraction of  $^{13}\text{CO}$ ) just before the switch ( $t = 0$ ) and long after the switch ( $t \rightarrow \infty$ ). The curve M (mixing) shown in Fig. 12a is the response obtained for a nonadsorbing gas (Ar) passing through the reactor containing the catalyst (5, 14). The area of the difference between the  $^{13}\text{CO}(\text{g})$  response and that of mixing (M) provides the amount of CO reversibly adsorbed on the catalyst surface. This is found to be  $\theta_{\text{CO}} = 0.9$ , corresponding to 60 s of CO/He reaction with the catalyst surface. At the end of the experiment described above (Fig. 12a), the reactor is flushed in He for 15 s, closed and cooled to 313 K. The feed is then changed to  $\text{H}_2$  and a TPR experiment is initiated (Fig. 12b) to measure the quantity of nonexchangeable adsorbed species using the  $^{12}\text{CH}_4$  production (the  $^{13}\text{CH}_4$  production was not measured). The amount of this nonexchangeable CO is found to be  $\theta = 0.18$ , and its chemical composition is discussed later. Note that a small amount of surface CO,  $\theta_{\text{CO}} = 0.01$ , desorbs during  $\text{H}_2$  reduction. Experiments with longer times in CO/He, such as 300 s, 900 s, and 1 h, resulted in the same  $^{13}\text{CO}(\text{g})$  response as that in Fig. 12a. Thus, the amount of exchangeable CO species stays almost constant after 60 s of CO/He reaction.

(3b) *FTIR analysis.* To study the kinds of adsorbed CO species which readily exchange or do not exchange with gaseous  $^{13}\text{CO}$  and which might contribute to the results of Fig. 12, transient FTIR experiments with  $^{12}\text{C}^{18}\text{O}$

isotope gas have been conducted. Figure 13, spectrum a, is obtained after treatment of the catalyst at 523 K for 260 s with CO/He, whereas spectrum b after treatment with  $\text{C}^{18}\text{O}/\text{He}$  according to the sequence CO/He (260 s)  $\rightarrow$  He (80 s)  $\rightarrow$   $\text{C}^{18}\text{O}/\text{He}$  (100 s). The IR bands at 2046, 1965, and 1909  $\text{cm}^{-1}$  observed after CO/He treatment are now shifted to lower wavenumbers after  $\text{C}^{18}\text{O}/\text{He}$  treatment; there is also a slight shift in the maximum of the broad band (a shift from 1815 to 1803  $\text{cm}^{-1}$ ). Note that this band appears to be more symmetric after the  $\text{C}^{18}\text{O}/\text{He}$  treatment. This result might be interpreted as due to the shift of the bridged CO species according to the isotopic exchange, whereas the species responsible for the shoulder at 1697  $\text{cm}^{-1}$  remain unaffected (not exchangeable species).

## DISCUSSION

The present work aimed to study in some detail *in situ* the interaction of CO with the surface of Rh/MgO catalyst in the range 300–573 K, using both transient FTIR and mass spectrometry. The use of these techniques allowed to identify the chemical composition of the adsorbed carbon species formed and to measure their surface coverages as a function of reaction temperature and time on stream in CO/He. In addition, the kinetics of hydrogenation of the adsorbed CO species as a function of catalyst pretreatment in different gas atmospheres has been studied, as well as the exchange properties of the adsorbed CO species with gaseous  $^{13}\text{CO}$ . These aspects are discussed in what follows.

(a) *Adsorbed carbon species formed after CO/He reaction in the range 300–523 K.* The transient FTIR results of Fig. 5 show that various adsorbed species with a CO chemical bond are formed following chemisorption of CO at 523 K on a reduced Rh/MgO surface at 623 K. The IR band at 2046  $\text{cm}^{-1}$  is attributed, according to various literature data (27, 40, 41), to the linear adsorbed CO species. Saturation of the sites which populate the linear CO species is rapid (within 30 s, Fig. 5). The IR band at 1822  $\text{cm}^{-1}$  is attributed, according to the literature (27, 40, 41), to the bridged adsorbed CO species, where its maximum surface coverage is rapidly obtained as in the case of linear CO species. The aforementioned IR bands due to linear and bridged CO species shift to higher wavenumbers, 2074 and 1878  $\text{cm}^{-1}$ , respectively, when chemisorption of CO is performed at 300 K (Fig. 6, curve a). The IR bands at 1966 and 1906  $\text{cm}^{-1}$  which appear as shoulders in Fig. 5, after interaction of CO with the catalyst surface at 523 K, are rarely reported in the literature over Rh-supported catalysts. This is probably related to the fact that in most of these studies adsorption of CO was recorded at 300 K, and as it is discussed below, under these conditions these IR bands are not observed.

The IR bands at 1966 and 1906  $\text{cm}^{-1}$  shown in Fig. 5

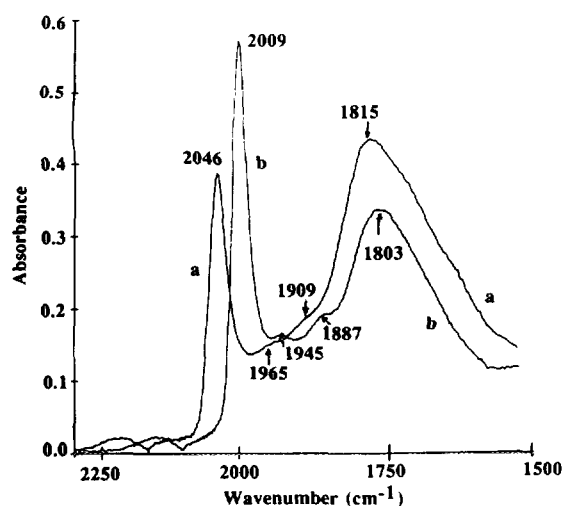


FIG. 13. FTIR spectra in the range 1500–2250  $\text{cm}^{-1}$  recorded at 523 K following CO chemisorption and isotopic exchange with  $\text{C}^{18}\text{O}$  as follows. Spectrum (a) is obtained after chemisorption of CO at 523 K for 260 s. Spectrum (b) is obtained at 523 K after  $\text{C}^{18}\text{O}/\text{He}$  treatment according to the sequence: CO/He (260 s)  $\rightarrow$  He (80 s)  $\rightarrow$   $\text{C}^{18}\text{O}/\text{He}$  (100 s).

cannot be attributed to adsorbed species on the support alone, since the FTIR results of Fig. 11 show only weak IR bands which correspond to carbonate species ( $1200\text{--}1500\text{ cm}^{-1}$ ). Chuang and Pien (42), in their study of CO adsorption over Rh/SiO<sub>2</sub> at 10 atm and 300 K and over a partially oxidized Rh surface, report IR bands at  $2078\text{ cm}^{-1}$  (linear CO species),  $1882\text{ cm}^{-1}$  (bridged CO species), and  $2038$  and  $2096\text{ cm}^{-1}$  (gem-dicarbonyl species on Rh<sup>+</sup> sites). The authors also noted shoulders at  $2007$  and  $1857\text{ cm}^{-1}$  which were not observed over the fully reduced Rh surface. It is also mentioned here that a shoulder at around  $1900\text{ cm}^{-1}$  can also be observed in the spectrum given by Chuang and Pien in Fig. 4 (42). These bands do not fit the IR spectrum of various CO/Rh organometallic complexes (43), and the authors leave the interpretation of these bands open. The aforementioned IR bands appear as shoulders over the Rh/SiO<sub>2</sub> case (42), and their relative intensities compared to those of linear and bridged CO species are similar to those observed over the present Rh/MgO catalyst after chemisorption at 523 K. We have no accurate interpretation of the structure and nature of adsorption sites responsible for these species. However, some information related to their formation can be obtained on the results of Fig. 7.

CO chemisorption at 300 K on a fully reduced Rh-supported surface leads to a classical FTIR spectrum with linear, bridged, and gem-dicarbonyl CO species, the latter easily formed over small Rh crystallites (18, 21–25). On the other hand, as previously mentioned the shoulders at  $1906$  and  $1966\text{ cm}^{-1}$  observed over the present catalyst (Fig. 5) are not usually observed. The FTIR spectrum recorded during TPD (Fig. 7b) shows that above 423 K the gem-dicarbonyl CO species disappear, while a shoulder at  $1918\text{ cm}^{-1}$  appears. At higher temperatures ( $T = 523\text{ K}$ ) two other shoulders at  $1894$  and  $1697\text{ cm}^{-1}$  appear (Fig. 9). These results seem to suggest that there exists some correlation between the disappearance of the gem-dicarbonyl CO species and the formation of the unknown species which give rise to the shoulders mentioned above. Thus, Rh<sup>+</sup> or other Rh<sup>n+</sup> species seem to be likely involved with CO chemisorbed states. In fact, recent XPS work on the present catalyst showed that after adsorption of CO at 523 K followed by TPD, part of the Rh surface is found to be partially oxidized (Rh<sup>n+</sup> species) (28). It might be suggested that such sites are along the interface formed by the small Rh crystallites and the surface of the MgO support, where an electron transfer is likely to take place. In conclusion, the present FTIR results suggest that at least five kinds of adsorbed species with CO bands are formed after interaction of CO at 523 K with the Rh/MgO surface reduced in H<sub>2</sub> at 623 K. Assuming that the extinction coefficients for all the five species are of the same order of magnitude (a difference by a factor in the range 3–5) (46), only two of them (linear and bridged CO species) are present in high surface coverages.

Estimation of the surface coverage of all the adsorbed CO species formed at 523 K as a function of time on stream in CO/He is obtained from the hydrogenation results of Fig. 1. These results clearly indicate that the Rh surface is completely covered with CO, and the surface coverage of it is independent of time in CO/He, in harmony with the FTIR results of Fig. 5; there are no major changes in the intensity of the bands where only a slight increase of the shoulder at  $1697\text{ cm}^{-1}$  from 60 s to 1 h in CO/He is observed. By increasing the adsorption temperature to 573 K, it is found that the surface coverage of adsorbed CO species decreases only slightly (Fig. 2). These results are similar to those found during CO/H<sub>2</sub> reaction over the present catalyst (4), but different from those observed over the 5 wt% Rh/Al<sub>2</sub>O<sub>3</sub> catalyst (2, 3). For the latter case, it was found that the surface coverage of CO decreases from  $\theta = 0.96$  to 0.6 in the range 453–533 K. Thus, chemisorption of CO on Rh/MgO appears to be stronger than on Rh/Al<sub>2</sub>O<sub>3</sub> in agreement with TPD studies over these catalysts (2, 29). Assuming that particle size effects on determining the adsorption behaviour of CO on Rh are not so important, it would be necessary to invoke metal–support effects to explain the large differences in the chemisorption of CO observed over the present Rh/MgO and that of Rh/Al<sub>2</sub>O<sub>3</sub> reported previously (2, 3). In fact, such effects were invoked to explain the differences observed in the rate constant,  $k$ , of the CO dissociation step during methanation over these two catalysts (4). However, before this conclusion is reached, particle size effects should be carefully considered. This is a work in progress to be reported elsewhere.

The rate profiles of methane formation during the isothermal hydrogenation of adsorbed carbon species formed after CO/He reaction at 523 K (Figs. 1 and 2) lead to additional information about the chemical composition of these species. First, for all the hydrogenation temperatures studied, there is an initial sharp peak (spike) for the rate of CH<sub>4</sub> formation during the first second of reaction. A comparison with the FTIR results of Fig. 10 obtained during the same hydrogenation process, leads to the conclusions that (a) no CO species reacts so fast and (b) the very active species hydrogenated to methane cannot be detected by FTIR. It is very likely that this species is carbidic carbon which is formed during CO interaction with Rh/MgO in the range 523–573 K via the dissociation of CO, in agreement with the CO<sub>2</sub> production measured by mass spectrometry. Its surface coverage is found to be very small ( $\theta = 0.01$ ).

(b) *Isothermal hydrogenation of adsorbed carbon-containing species formed after CO/He reaction in the range 523–573 K.* Figure 1, curve (A) shows that during isothermal hydrogenation at 523 K, following CO/He reaction at 523 K, after the first sharp CH<sub>4</sub> peak due to reduction of active elementary carbon, the rate of CH<sub>4</sub>

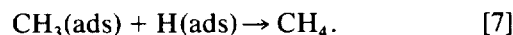
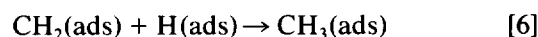
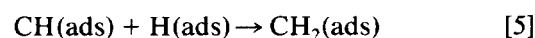
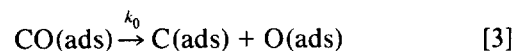
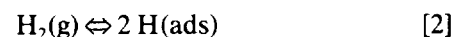
production increases slowly producing the beginning of a broad peak. At this temperature ( $T = 523$  K), the time  $t_m$  of the appearance of the maximum of this broad peak is higher than 3 min (see Fig. 1, beginning of the TPR of adsorbed species). A small shoulder may be observed at about 30 s on stream in  $H_2$ . For higher temperatures (Fig. 2) the  $CH_4$  peak maximum is well observed (curves B and C), and the time  $t_m$  of the appearance of this peak maximum decreases with increasing hydrogenation temperature. When an oxygen treatment of the catalyst sample at 623 K followed by  $H_2$  reduction is applied, the maximum is also well observed even at a lower temperature (curve A, Fig. 4). Comparison of the curves A–C of Fig. 1 and curves A–C of Fig. 4 indicates that the increase of the time on stream in CO/He leads to a decrease in the rate of  $CH_4$  production and, therefore, to an increase in the time of appearance of the peak maximum (compare curves A and B in Fig. 4). The FTIR results obtained indicate that during this period of hydrogenation only the CO adsorbed species (mainly the linear and bridged species) are hydrogenated (Fig. 10). In addition, the present FTIR results show that the time on stream in CO/He only slightly affects the nature of the adsorbed CO species (Figs. 5 and 8).

Based on the above discussion, the main point that has to be explained is the fact that during isothermal hydrogenation a peak of  $CH_4$  can be formed. In previous publications (35–37) related to the isothermal hydrogenation of adsorbed carbon species formed on an Fe/ $Al_2O_3$  catalyst after CO/He or CO/ $H_2$  reaction, it has been shown by kinetic models that the transient response of the  $CH_4$  formation can give more insight into the elementary processes of the hydrogenation reaction, and, therefore, to permit a more accurate characterization of the adsorbed species. In the case of CO/He reaction on Fe/ $Al_2O_3$  catalyst (33), the isothermal hydrogenation of the carbonaceous species leads to a decreasing exponential-like response independent of the temperature of hydrogenation used (473–573 K). This behaviour has been explained by invoking the presence of one rate-limiting step in the sequence of steps for the hydrogenation process to form  $CH_4$ . However, on the present Rh/MgO catalyst the  $CH_4$  responses are different and peaks with  $t_m \neq 0$  are observed. The main difference between the two catalysts (Fe/ $Al_2O_3$  and Rh/MgO) with respect to the CO/He reaction at high temperatures, is the stability of the CO adsorbed species (linear and bridged) on the Rh/MgO, as evidenced by the He treatment results of Figs. 3 and 9. This means that formation of  $CH_4$  from these CO species involves a dissociation step which was not of concern over the Fe/ $Al_2O_3$  catalyst, since the surface coverage of CO was found to be practically zero. On the Fe/ $Al_2O_3$  catalyst the hydrogenation process concerns elementary carbon formed on the iron surface. It is noted here that

the first sharp peak of  $CH_4$  observed in Figs. 1 and 2 is attributed to elementary carbon, the hydrogenation of which produces an exponentially decreasing  $CH_4$  response, in agreement with the results obtained on the Fe/ $Al_2O_3$  catalyst (33).

On the present Rh/MgO catalyst the main part of the  $CH_4$  response arises from the hydrogenation of adsorbed CO species. Thus, at least two elementary steps must be considered: the dissociation of CO followed by the hydrogenation of elementary carbon. A short presentation of a kinetic model which supports the interpretation of the present experimental results shown in Figs. 1, 2, and 4 is given in what follows. More details of this analysis and experimental results which verify it are presented elsewhere (44).

Considering one kind of adsorbed CO species (linear or bridged), and assuming first order kinetics for the dissociation step of CO, the elementary steps for the hydrogenation of adsorbed CO to  $CH_4$  can be written as follows:



In the above described sequence of steps the desorption step of adsorbed CO is neglected, based on the experimental results of Figs. 1–4, where during hydrogenation very little CO desorbs ( $\theta_{CO} < 0.01$ ). Assuming that steps [5]–[7] are much faster than steps [3] and [4], then the rate of  $CH_4$  production,  $\Phi$ , as a function of time of hydrogenation is given as

$$\Phi = k_1 C(ads) H(ads), \quad [8]$$

where  $C(ads)$  and  $H(ads)$  are the surface concentrations of elementary carbon and adsorbed hydrogen at time  $t$  of the isothermal hydrogenation experiment. Assuming that adsorption of  $H_2$  (1 bar  $H_2$ ) is rapidly obtained during the first seconds of the hydrogenation (step [2] is in equilibrium), it is assumed then that  $H(ads) = H$  remains constant during the hydrogenation process. The surface concentration of hydrogen is assumed to be given by the Langmuir equation as

$$H = ((\sqrt{KP}) / (1 + \sqrt{KP})) H_0, \quad [9]$$

where  $K$  is the equilibrium constant for  $H_2$  adsorption and  $H_0$  is the concentration of available sites for hydrogen chemisorption.

The evolution of  $\Phi$  with time of hydrogenation is given by Eq. [10] after solution of the ordinary differential equations described elsewhere (44) and using  $C(\text{ads})^\circ = 0$  at  $t = 0$  as

$$\Phi = k_1 k_0 \text{HCO}^\circ(\text{ads}) (\exp(-k_1 H t) - \exp(-k_0 t)) / (k_0 - k_1 H), \quad [10]$$

where  $\text{CO}^\circ(\text{ads})$  is the initial surface concentration of the CO species.

The rate of  $\text{CH}_4$  formation,  $\Phi$ , presents a maximum with respect to the time of hydrogenation ( $d\Phi/dt = 0$ ) given as

$$t_m = (\ln(k_1 H / k_0)) / (k_1 H - k_0). \quad [11]$$

It appears from Eq. [11] that whatever is the magnitude of  $k_1 H$ , and  $k_0$ ,  $t_m$  is always positive, and thus a maximum may be observed if the value of  $k_1 H$ , or  $k_0$  is not too large (for large values,  $t_m$  is lower than 1 s and this behaviour will be recorded as an exponential decay response).

The results of Fig. 3, curves a and b, clearly suggest that the rate of dissociation of CO under He flow is very slow at 523 K, since a slight only increase of the first peak of  $\text{CH}_4$  response (spike at  $t = 0$  of  $H_2$  switch) is observed after 10 min on stream in He. It might be considered that  $k_1 H > k_0$  (i.e.  $k_1 H = 100 k_0$ ). After using this assumption in Eq. [11], Eq. [12] is obtained:

$$t_m = (\ln(k_1 H / k_0)) / k_1 H. \quad [12]$$

Considering some reasonable values for the parameters,  $H = 10^{13}$  sites/cm<sup>2</sup>,  $k_1 = A \exp(-E_r/RT)$  with  $A = 10^{-2}$  (cm<sup>2</sup>/site-sec) and  $E_r = 130$  KJ/mol, and  $T = 553$  K, a value of  $t_m = 85$  s is obtained from Eq. [12]. This value is of the order of the experimental value observed (Fig. 2, curve B). Considering now that two or more CO species with different activation energies of hydrogenation and dissociation are present on the surface, their hydrogenation should give various peaks. This explains the existence of shoulders on the  $\text{CH}_4$  response in Fig. 4, curve A, and Fig. 2, curve B, which may correspond to hydrogenation of linear and bridged CO species. The expression of  $t_m$  given by Eq. [12] predicts also that the increase of temperature leads to a decrease of  $t_m$ , a result which is observed in Fig. 2.

The increase of the time of the appearance of the peak maximum with time on stream in CO/He (Fig. 1) remains to be explained, and this is done in what follows. As the nature of the adsorbed CO species and their coverages do not change with time on stream (Figs. 1, 5, and 8), it

is reasonable to assume that their activation energy of dissociation is constant. The shift of the peak maximum with time on stream in CO/He may only then be interpreted by a decrease in the number of hydrogen sites,  $H_0$  (see Eq. [9]). A study of  $d(t_m)/d(H)$  shows that if the value of  $H$  is greater than  $(2.3 k_0/k_1)$ , then if  $H$  decreases  $t_m$  increases (the condition of  $H > (2.3 k_0/k_1)$  can be easily satisfied under experimental conditions). Thus, the increase of the value of  $t_m$  must be associated with the decrease in the value of  $H$  due to some poisoning or disappearance of  $H_2$  chemisorption sites,  $H_0$ , with time on stream in CO/He. The decrease of the  $H_0$  value explains also the shift of the maximum of the  $\text{CH}_4$  peak during TPR (Fig. 1) with time on stream in CO/He (36).

The comparison of the results obtained after oxygen treatment of the catalyst (Fig. 4, curve A) and those after CO/He treatments followed by  $H_2$  reduction (Fig. 4, curves B and C) indicate that this increase in the  $t_m$  value with time on stream in CO/He cannot be altered by  $H_2$  reduction at 623 K. Only oxygen treatment at 623 K before  $H_2$  reduction can give the initial  $\text{CH}_4$  peak with a  $t_m$  value at 523 K lower than 3 min (Fig. 4, curve A). It is suggested that the decrease of the hydrogen sites ( $H_0$ ) with time on stream in CO/He may be related to a poisoning of the sites by carbon species formed during  $H_2$  TPR (Fig. 4) and which cannot be removed by  $H_2$  at 723 K. The fact that  $\text{CO}_2$  was found to be formed during oxygen treatment at 623 K supports this idea. Previous work on the effects of oxygen treatment of the present catalyst, after various CO/He reactions, on  $H_2$  chemisorption at 310 K shows that hydrogen sites can be poisoned by inactive carbon not hydrogenated at 723 K (29). It could also be speculated here whether some morphological changes in the Rh particles during oxygen treatment of the catalyst surface at 623 K might lead to an increase in the number of  $H_0$  sites, thus increasing the rate of hydrogenation of CO (compare Fig. 4, curve A, and Fig. 1, curve A). Such morphological changes in the microstructure of Rh-supported surface has been reported (45). In addition, a related result to the above mentioned change in the catalyst surface with oxygen treatment can be found in Fig. 6, where adsorption of CO at room temperature on a used catalyst does not form gem-dicarbonyl CO species, a result opposite to that obtained on a fresh catalyst sample.

Summarizing the aspects of the kinetics of hydrogenation of CO over the present Rh/MgO catalyst, the following are noted. Methane production from the hydrogenation of adsorbed CO species proceeds with a mechanism which is controlled by two steps, the dissociation of CO and the hydrogenation of the adsorbed carbon species derived. The former step appears to be the slowest step of the process, thus much controlling the overall reaction rate. The shoulder appeared in the  $\text{CH}_4$  response of Fig. 4, curve A arises from the presence of more than one CO

species (linear and bridged), and the increase of the  $t_m$  value with time on stream in CO/He is the result of a decrease of hydrogen chemisorption sites,  $H_0$ , either by poisoning with inactive carbon (graphite-like) or by some reconstruction of the Rh particles by oxygen treatment at 623 K. The former explanation seems to be the most likely based on some experimental evidence.

(c)  $^{13}\text{CO}$  exchange reaction. The experiment of exchange of CO species with  $^{13}\text{CO}$  (Fig. 12) shows that most of the adsorbed CO species are exchangeable (85%) after 60 s of reaction in CO/He. This result agrees well with the FTIR results which indicate that linear and bridged CO species, as well as the undetermined species which gives shoulders at 1965 and 1909  $\text{cm}^{-1}$  are exchangeable. The nonexchangeable CO species seem to correlate with the shoulder initially formed at 1697  $\text{cm}^{-1}$  since after the  $\text{C}^{18}\text{O}$  exchange the IR bands of the bridged CO species seem more symmetrical. It is speculated here that such a CO species may be of a bridged type associated with the Rh metal and the MgO surfaces. It is interesting to mention here also that a CO species with similar behaviour as far as exchange with  $^{13}\text{CO}$  has been observed during CO/ $\text{H}_2$  reaction over the present catalyst (4). This species was found to participate in the mechanism of  $\text{CH}_4$  formation at 573 K. The latter result is in agreement with the TPR results of Fig. 12b.

### CONCLUSIONS

The following conclusions are derived from the present work.

(1) Chemisorption of CO at 523 K over a 2.5 wt% Rh/MgO catalyst results mainly in the formation of linear and bridged CO species as evidenced by FTIR. An FTIR band at 1697  $\text{cm}^{-1}$  is found to likely be correlated with the formation of another strongly bound CO species along the metal-support interface, but in small amounts. Two other undetermined in structure CO species are also observed (IR bands at 1906 and 1966  $\text{cm}^{-1}$ ) but also in very small amounts. Formation of gem-dicarbonyl CO species at 523 K does not take place, but its formation at 300 K is found to strongly depend on the catalyst history of pretreatment with CO/He.

(2) Reaction of the catalyst surface with 10 mol% CO/He in the range 523–573 K between 60 and 900 s results only in a small amount of elementary carbon, while it is found that the surface is fully covered by undissociated CO species.

(3) Exchange experiments with  $^{13}\text{CO}$  and  $\text{C}^{18}\text{O}$  at 523 K, following CO/He reaction, show that only the linear and bridged CO species readily exchange.

(4) Hydrogenation of adsorbed CO species to form  $\text{CH}_4$  proceeds with two elementary steps which are considered

to control the overall process. These are the dissociation of CO and the hydrogenation of the carbon species derived. The kinetic model developed explains the main experimental observations related to the presence of a  $\text{CH}_4$  peak during isothermal hydrogenation of adsorbed CO species.

(5) The number of hydrogen chemisorption sites is found to decrease with time on stream in CO/He at 523 K followed by  $\text{H}_2$  TPR to 723 K, as evidenced by transient hydrogenation experiments. Inactive carbon, not hydrogenated to  $\text{CH}_4$  at 723 K, is considered to be the most likely event to explain this behaviour.

### ACKNOWLEDGMENTS

Support of this work was provided by the National Science Foundation through Grant CBT-8517158, by the University of Connecticut Research Foundation, and by NATO Exchange Program 85/0669.

### REFERENCES

- Happel, J., "Isotopic Assessment of Heterogeneous Catalysis." Academic Press, New York, 1986.
- Efstathiou, A. M., and Bennett, C. O., *J. Catal.* **120**, 118 (1989), and references therein.
- Efstathiou, A. M., and Bennett, C. O., *J. Catal.* **120**, 137 (1989).
- Efstathiou, A. M., *J. Mol. Catal.* **67**, 229 (1991).
- Stockwell, D. M., Chung, J. S., and Bennett, C. O., *J. Catal.* **112**, 135 (1988).
- Stockwell, D. M., and Bennett, C. O., *J. Catal.* **110**, 354 (1988).
- Stockwell, D. M., Bianchi, D., and Bennett, C. O., *J. Catal.* **113**, 13 (1988).
- Mims, C. A., and McCandlish, L. E., *J. Phys. Chem.* **91** (4), 929 (1987), and references therein.
- DePontes, M., Yakomizo, G. H., and Bell, A. T., *J. Catal.* **104**, 147 (1987).
- Zhou, X., and Gulari, E., *J. Catal.* **105**, 499 (1987), and references therein.
- Winslow, P., and Bell, A. T., *J. Catal.* **94**, 385 (1985), and references therein.
- Siddall, J. H., Miller, M. L., and Delgass, W. N., *Chem. Eng. Commun.* **83**, 261 (1989).
- Balakos, M. W., Chuang, S. S. C., and Srinivas, G., *J. Catal.* **140**, 281 (1993).
- Efstathiou, A. M., Ph.D. thesis, University of Connecticut, 1989.
- Bianchi, D., Tau, L. M., Borcar, S., and Bennett, C. O., *J. Catal.* **84**, 358 (1983).
- Underwood, R. P., and Bennett, C. O., *J. Catal.* **86**, 245 (1984).
- Zhou, X., and Gulari, E., *Langmuir* **2**, 709 (1986).
- Dictor, R., and Roberts, S., *J. Phys. Chem.* **93**, 2526 (1989).
- Efstathiou, A. M., Chafik, T., Bianchi, D., and Bennett, C. O., in "Proceedings, 10th International Congress on Catalysis, Budapest, 1992." (L. Gucci, F. Solymosi, and P. Tetenyi, Eds.), p. 1563. Akadémiai Kiadó, Budapest.
- Yokomizo, G. H., and Bell, A. T., *J. Catal.* **119**, 467 (1989) and references therein.
- Buchanan, D. A., Hernandez, M. E., Solymosi, F., and White, J. M., *J. Catal.* **125**, 456 (1990).

22. van't Blik, H. F. J., van Zon, J. B. A. D., Huizinga, T., Vis, J. C., Koningsberger, D. C., and Prins, R., *J. Phys. Chem.* **87**, 2264 (1983).
23. Solymosi, F., Rasko, J., and Bontovics, J., *Catal. Lett.* **19**, 257 (1993) and references therein.
24. Zaki, M. I., Kunzmann, G., Gates, B. C., and Knozinger, H., *J. Phys. Chem.* **91**, 1486 (1987).
25. Basu, P., Panayotov, D., and Yates, J. T., Jr., *J. Phys. Chem.* **91**, 3133 (1987).
26. van der Lee, G., and Ponec, V., *J. Catal.* **99**, 511 (1986).
27. Tanaka, Y., Iizuka, T., and Tanabe, K., *J. Chem. Soc. Faraday Trans. 1* **78**, 2215 (1982).
28. Efstathiou, A. M., Tan, B. J., and Suib, S. L., *J. Catal.* **140**, 564 (1993).
29. Efstathiou, A. M., *J. Mol. Catal.* **69**, 41 (1991).
30. Chafik, T., Khalfallah, M., Bianchi, D., and Gass, J. L., submitted for publication.
31. Bennett, C. O., in "Catalysis under Transient Conditions" (A. T. Bell and L. L. Hegedus, Eds.), American Chemical Society Symposium Series, Vol. 178, p. 1. Amer. Chem. Soc., Washington D. C. 1982.
32. Winslow, P., and Bell, A. T., *J. Catal.* **86**, 158 (1984).
33. (a) Bianchi, D., Borcar, S., Teule-Gay, F., and Bennett, C. O., *J. Catal.* **82**, 442 (1983); (b) Bianchi, D., Tau, L. M., Borcar, S., and Bennett, C. O., *J. Catal.* **84**, 358 (1983).
34. Underwood, R. P., and Bennett, C. O., *J. Catal.* **86**, 245 (1984).
35. Bianchi, D., and Gass, J. L., *J. Catal.* **123**, 298 (1990).
36. Bianchi, D., and Gass, J. L., *J. Catal.* **123**, 310 (1990).
37. Ahlafi, H., Bennett, C. O., and Bianchi, D., *J. Catal.* **133**, 83 (1992).
38. Rodionova, T. A., Tsyganenko, A. A., and Filimonov, V. N., *Adsorbts. Adsorbenty* **10**, 33 (1982).
39. Garrone, E., Zecchina, A., and Stone, F. S., *J. Chem. Soc. Faraday Trans. 1* **84**(8), 2843 (1988).
40. Yates, J. T., Duncan, T. M., Worley, S. D., and Vaughan, R. W., *J. Chem. Phys.* **70**, 1219 (1979).
41. Worley, S. D., Rice, C. A., Mattson, G. A., Curtis, C. W., Guin, J. A., and Tarrer, A. R., *J. Chem. Phys.* **76**, 20 (1982).
42. Chuang, S. S. C., and Pien, S. I., *J. Catal.* **135**, 618 (1992).
43. Pino, P., Piacenti, F., and Bianchi, M., in "Organic Synthesis via Metal Carbonyls" (I. Wender and P. Pino, Eds.), Vol. 2, p. 43. Wiley, New York, 1977.
44. Efstathiou, A. M., Bianchi, D., and Bennett, C. O., submitted for publication.
45. Lee C., and Schmidt, L. D., *J. Catal.* **101**, 123 (1986).
46. Rasband, P. B., and Hecker, W. C., *J. Catal.* **139**, 551 (1993).